Imaging of photonic modes in an AlN-based photonic crystal probed by an ultra-violet internal light source

C. Brimont,[1,2] T. Guillet,[1,2,*] S. Rousset,[1,2] D. Néel,[3] X. Checoury,[3] S. David,[3] P. Boucaud,[3] D. Sam-Giao,[4] B. Gayral,[4] M. J. Rashid,[5] and F. Semond[5]

[1]Université Montpellier 2, Laboratoire Charles Coulomb UMR 5221, F-34095 Montpellier, France

[2]CNRS, Laboratoire Charles Coulomb UMR 5221, F-34095 Montpellier, France

[3]Institut d'Électronique Fondamentale, UMR CNRS 8622, Université Paris Sud-11, F-91405 Orsay, France

[4]CEA-INAC, 17 rue des Martyrs, 38054 Grenoble, France

[5]CRHEA–CNRS, Rue Bernard Grégory, F-06560 Valbonne, France

*Corresponding author: thierry.guillet@univ-montp2.fr

The spatial distribution of photon modes confined in a 0D cavity and a 1D W1 waveguide is investigated on AlN-based photonic crystal (PC) membranes by spectrally resolved scanning confocal microscopy in the ultra-violet spectral range. The influence of the fabrication-induced disorder of the PC on the photon modes is analyzed. The cavity modes are shown to be robust with respect to disorder, whereas the 1D modes of the W1 waveguide are localized near its cut-off frequency. Those modifications of the lowest energy photonic modes are compared to simulations of weakly disordered photonic structures. © 2013 Optical Society of America

OCIS codes: (350.4238) Nanophotonics and photonic crystals; (180.1790) Confocal microscopy; (300.6470) Spectroscopy, semiconductors.

http://dx.doi.org/10.1364/OL.38.005059

The propagation of light in a photonic crystal (PC) waveguide and its coupling to a cavity is attracting a strong interest related to the potential applications in the field of integrated photonics. It is strongly sensitive to the photonic disorder related to the imperfections of the fabrication processes [1,2]. One possible effect of photonic disorder is to scatter light out of guided modes, leading to propagation losses. For guided modes in the slow light regime, near the cut-off frequency of the waveguide, the sensitivity to photonic disorder becomes larger and it can, in particular, lead to the formation of localized photonic states due to coherent backscattering [3,4]. A wide range of techniques have been developed to probe the photonic disorder and the induced density of states of photonic modes. Its main signature lies in the attenuation observed in the transmission spectroscopy of waveguides [5]. Disorder-induced light scattering and back-scattering has been studied in detail by specific techniques such as optical low-coherence reflectometry for dispersive Bloch modes [6]. Closer to the band edge of the waveguide, partially localized photonic modes have first been probed by injecting light in the waveguide and imaging the out-of-plane scattered light [7]. Such techniques based on light injection allow distinguishing dispersive/ballistic and diffusive regimes of propagation [3], but they are insensitive to strongly localized photonic modes at the onset of the band edge and their contribution to the local density of states (LDOS). Probing those last modes usually requires scanning near-field optical microscopy (SNOM) based on passive probes [8,9] or on probes with a single emitter or a nanoantenna at their ends [10,11]. However SNOM techniques have essentially been employed for the imagery of confined modes in cavities, especially because the proximity of the probe and the PC induces energy shifts and slight modifications

of the LDOS [9] that can be comparable to the effect of the intrinsic disorder. Cathodoluminescence has also been applied to the imagery of cavity modes [12] with enhanced spatial resolution. Photoluminescence has rarely been used to simultaneously perform the spectroscopy of PC waveguides and image the localized modes [13–17]. Currently, it is mainly exploited for the study of a single dot coupled to a cavity [18].

In this Letter we investigate both the confined modes in a cavity and the localized modes at the band edge of a W1 waveguide through confocal microscopy. The investigated PC samples are based on III-N semiconductor materials, whose application to photonics is attracting a growing interest for its wide transparency spectral range, from the infrared [19] to the visible [20] and near ultraviolet (UV) [21–26]. GaN quantum dots embedded in the PC membrane are used as a broadband internal light source with a very low absorption and an efficient emission in the blue and UV at room temperature. We have performed scanning confocal microscopy of a bare W1 waveguide and a series of cavities with increasing confinement in order to image the cavity (0D) and waveguide (1D) photonic modes. The use of internal emitters allows one to work on waveguides free of input and output couplers and avoid the use of a UV tunable laser source. The precise mapping of each photonic mode provides evidence of the interplay between the modes confined in the cavity and the waveguide in the presence of a shallow disorder. Those modes are analyzed with finite difference time-domain (FDTD) simulations. Compared to recent studies of the LDOS in photonic structures [8–11,13, 15,17], an additional specificity of the present work lies in the addressed UV spectral range. This implies the achievement of high-quality photonic membranes with short period and hole diameters, as well as the

development of a high-resolution noncommercial microscope dedicated to the UV range.

The present sample is based on an AlN-on-Si membrane. We have designed AlN nanocavities obtained by a small width modulation of a slab PC W1 waveguide for operation in the near UV ($\lambda = 300$ nm–400 nm). Their fabrication and the assessment of large quality factors in this spectral range (up to $Q = 4400$ at 395 nm) has been described in previous works [24,26]. Within the W1 waveguide, the cavities are obtained by slightly displacing 30 holes away from the waveguide center, as proposed in [27]. The present study focuses on a series of cavities based on the same W1 waveguide (PC lattice period $a = 150$ nm, hole radius $r/a = 0.27$) and with varying amplitudes d for the width modulation defining the cavity.

Figure 1 presents the microphotoluminescence (µPL) spectra recorded at room temperature when the exciting CW laser ($\lambda = 266$ nm) is focused at the center of the cavity, and the emission is collected at normal incidence through the microscope objective (numerical aperture 0.4). As analyzed in [26], those spectra consist of two families of peaks corresponding to the even and odd modes supported by the W1 waveguide. Each family presents a 0D mode at low energy and a few 1D modes of the W1 waveguide at higher energies. The even 1D modes are observed in the same spectral range (3.18–3.20 eV) for all values of the displacement amplitude d, including the case of the bare waveguide without a cavity ($d = 0$). As expected, the energy of the even 0D mode decreases as the displacement d is increased, a signature of an increasing confinement in the cavity.

To obtain the spatial distribution of the emission of each of the modes identified in Fig. 1, we have performed spectrally resolved scanning confocal microscopy. The emission is carefully imaged on the entrance slit of the spectrometer (Jobin Yvon iHR550), which is then imaged

on its CCD detector (32× magnification from sample to CCD). Scanning confocal microscopy usually refers to focusing the excitation laser and filtering the emission from the excitation spot with a pinhole in a plane conjugated to the sample; the investigated spot is then scanned on the sample. In the present case, the sample image is formed on the entrance slit of the spectrometer and the spatial filtering is obtained horizontally by closing the slit to 20 µm, and vertically by selecting only two CCD rows among the overall signal, corresponding to a spatial filter of 0.7 µm × 1.5 µm in the following images. The sample is scanned by 0.25 µm steps. Figure 2 presents different projections of such an image measured for the $d = 12$ nm cavity [Figs. 2(b) and 2(c)] and the waveguide [$d = 0$, Fig. 2(d)]. The scanning electron microscopy (SEM) image of a W1 waveguide is provided in Fig. 2(a). On the same scale, Fig. 2(b) presents the confocal signal measured at the energy of the even cavity mode at 3.135 eV. The signal is closely confined at the center of the cavity, and its full width (1.4 µm × 1.0 µm FWHM) reflects the confocal resolution, mainly related to the laser spot size. The spatial filtering is however, crucial to reject resonant scattered light and to reach such a resolution.

The spatial profile of all modes along the y-direction is then shown on the spectrally resolved image [Fig. 2(c)], as well as three spectra recorded at 0, ± 2 µm from the center of the PC. The 0D even and odd modes are confined around $y = 0$. On the contrary, the modes associated to the W1 waveguide (from 3.18 to 3.20 eV) are observed over the whole PC length, but they are not delocalized. Let us point out that the limited length (6.8 µm) of each PC pattern prevents us from considering them as infinitely long W1 waveguides: in an ideal structure, the 1D modes should consist in a series of Fabry–Perot resonances with a quantification energy of a few meV, delocalized over the whole waveguide. Our spectrally resolved images show that they rather form a continuum of partially localized states. Similar localized states are also observed on the bare W1 waveguide [Fig. 2(d)], especially at 0 and −2 µm positions. Their energy splitting reveals the typical amplitude of the fluctuations of the confinement potential along the waveguide of the order of 10 meV.

We should emphasize that our technique is essentially sensitive to localized states, with strong components around $k_y = 0$, due to the collection of the emission at normal incidence within the relatively small numerical aperture of our objective. This is very different from other imaging techniques based on the scattering of propagating light, where large k_y modes can be scattered within the collection solid angle and efficiently measured. Our technique therefore probes a specific type of disorder related to the inhomogeneities of hole positions and radii, leading to the observed localization of photon modes and the subsequent modification of their spectrum due to confinement. The intensity fluctuations of a given mode along the waveguide are attributed to scattering defects (local roughness, etching residuals, cracks). Other types of disorder and imperfections, such as the verticality of the hole sidewalls responsible for propagation losses on long distances due to TE–TM coupling, are not probed by our technique.
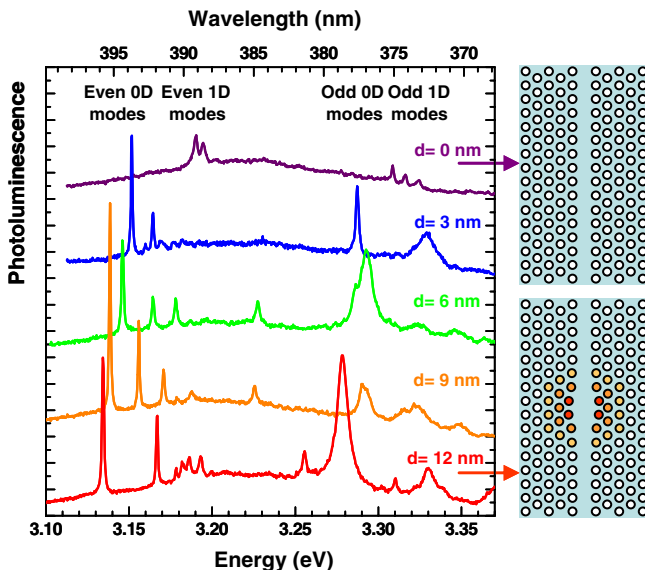

Fig. 1. Microphotoluminescence (µPL) spectra of a series of cavities with increasing modulation d, measured at the center of the cavity ($T = 300$ K). The geometry of the bare W1 waveguide ($d = 0$) and the cavities ($d = 3$–12 nm) are also illustrated; the red, orange and yellow circles correspond to lateral translations of the holes by d, $2d/3$, and $d/3$, respectively.
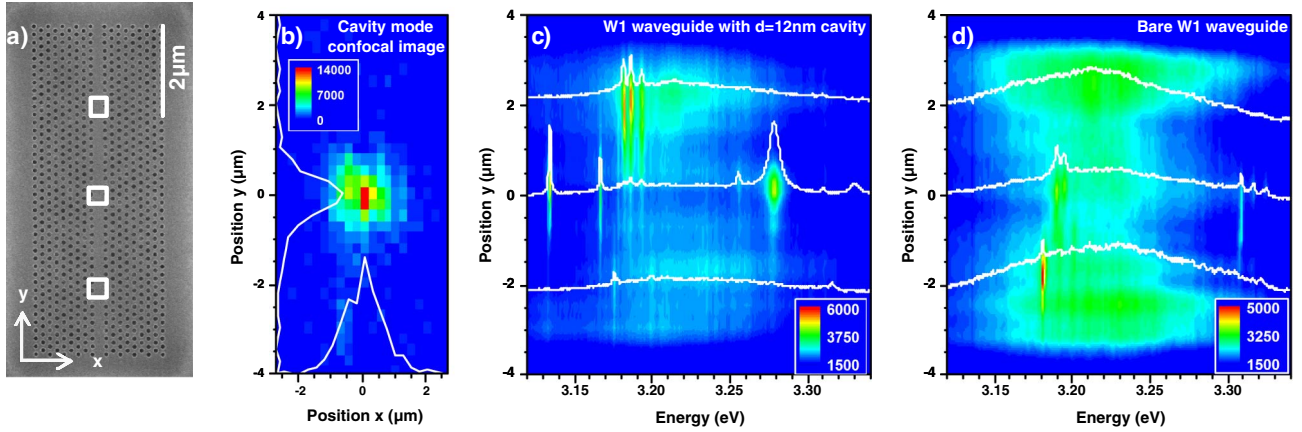
Fig. 2. (a) SEM image of a W1 PC waveguide with a cavity; the three squares indicate the positions where the spectra are measured. (b) Confocal image of the even cavity mode ($d = 12$ nm) at 3.135 eV, with the corresponding horizontal and vertical intensity profiles. (c), (d) Spatially and spectrally resolved PL signal (in counts/s) as the excitation spot is scanned along the waveguide at $x = 0$, for the $d = 12$ nm cavity and the bare W1 waveguide.

Let us now discuss more precisely the effect of disorder on the quality factor of the confined photon modes [26]. Figure 1 shows that the shallowest fabricated cavity, with a displacement amplitude of only $d = 3$ nm, confines a 0D mode at its center; this shows that the disorder is not dominating the intentional confinement. The measured quality factors, of the order of 2000–2700, are not strongly affected by the disorder. This confirms earlier theoretical predictions [28] showing that confined light modes are relatively immune to photonic disorder up to large disorder amplitudes, whereas the propagation (dispersive or diffusive) and localization of 1D modes near the waveguide cut-off frequency is the most prominent signature of photonic disorder [3].

The cavity presented in Figs. 2(a)–2(c) has been designed to support only one confined mode. However, a second confined even mode is observed at 3.165 eV, which was not expected. Similar appearances of additional confined modes are observed on most of our cavities, as shown by the four cavity spectra presented in Fig. 1. In order to quantify the role of fabrication disorder on the cavity confinement, FDTD simulations of slightly disordered cavities have been performed. The FDTD spectrum of a comparable ideal bare W1 waveguide is presented in Fig. 3, showing the Fabry–Perot quantization of the 1D states with a typical energy of ~5meV. Two cavities are also simulated for $d = 12$ nm, with and without disorder. Compared to the nominal cavity, the artificial disorder consists in a displacement by 4 nm of two additional holes on each side of the cavity (inset of Fig. 3). This displacement is sufficient to trap a second confined mode at the center of the waveguide (3.165 eV), and to enhance light extraction by 1D modes above 3.17 eV. This additional displacement corresponds to an extension of the confinement potential and the occurrence of higher-order localized modes. For larger disorder-related displacements, the spectroscopy of the waveguide and this cavity are more strongly affected and cannot be compared anymore with our observations.

To conclude, we have investigated the photonic modes in cavities and W1 waveguides within an AlN PC membrane. Confocal imagery allows us to observe the

strongly localized modes that are usually not accessible by transmission-based experiments. Slight modification of the spectrum of confined states in each cavity are also analyzed and compared with simulations of slightly modified cavities. We observe that small fluctuations of the PC hole distribution are not precluding the possibility to efficiently trap photons in the cavities, but they strongly
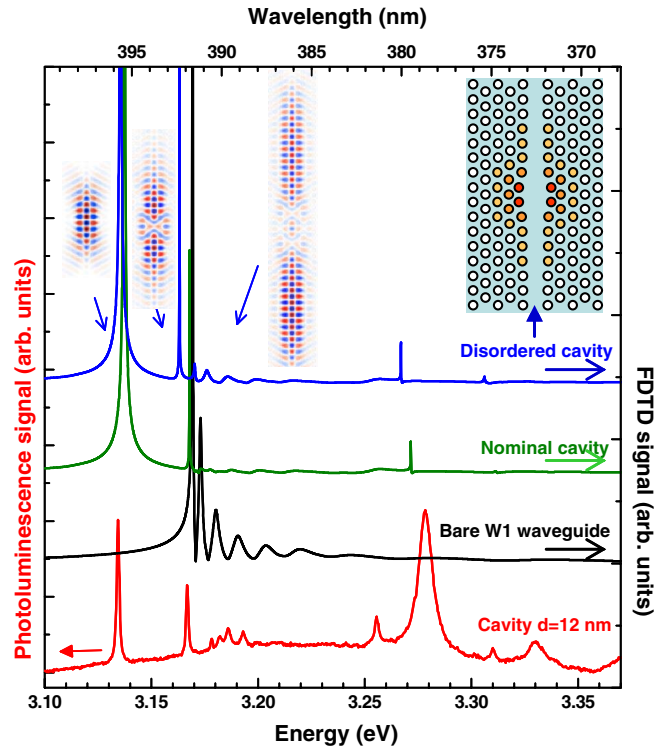

Fig. 3. PL signal of the $d = 12$ nm cavity (bottom); 3D-FDTD signal obtained from the local field profile for the W1 waveguide, the nominal cavity, and the slightly disordered cavity (see text). The vertical scale is adjusted to emphasize the excited modes. The diagrams above the graph show 3D-FDTD simulations for the H_z component of the field of the two confined cavity modes and the first delocalized mode for the disordered cavity, as well as an illustration of the artificially disordered cavity, with the same color conventions as in Fig. 1.

modify the spatial distribution of excited modes in the cavity and the waveguide. The imaging of confined modes in the UV range appears as a powerful technique to analyze nitride PCs. This method brings useful information to understand the spectral response of nitride photonic integrated devices and in turn optimize their design for UV applications.

References

1. S. Hughes, L. Ramunno, J. F. Young, and J. E. Sipe, Phys. Rev. Lett. **94**, 033903 (2005).
2. J. Topolancik, F. Vollmer, R. Ilic, and M. Crescimanno, Opt. Express **17**, 12470 (2009).
3. N. Le Thomas, H. Zhang, J. Jagerska, V. Zabelin, R. Houdré, I. Sagnes, and A. Talneau, Phys. Rev. B **80**, 125332 (2009).
4. M. Patterson and S. Hughes, J. Opt. **12**, 104013 (2010).
5. S. Mazoyer, P. Lalanne, J. Rodier, J. Hugonin, M. Spasenovic, L. Kuipers, D. Beggs, and T. Krauss, Opt. Express **18**, 14654 (2010).
6. A. Parini, P. Hamel, A. D. Rossi, S. Combrié, N.-V.-Q. Tran, Y. Gottesman, R. Gabet, A. Talneau, Y. Jaouën, and G. Vadalà, J. Lightwave Technol. **26**, 3794 (2008).
7. J. Topolancik, B. Ilic, and F. Vollmer, Phys. Rev. Lett. **99**, 253901 (2007).
8. G. Colas des Francs, C. Girard, J.-C. Weeber, and A. Dereux, Chem. Phys. Lett. **345**, 512 (2001).
9. F. Intonti, S. Vignolini, F. Riboli, A. Vinattieri, D. S. Wiersma, M. Colocci, L. Balet, C. Monat, C. Zinoni, L. H. Li, R. Houdré, M. Francardi, A. Gerardino, A. Fiore, and M. Gurioli, Phys. Rev. B **78**, 041401 (2008).
10. S. Kühn, C. Hettich, C. Schmitt, J.-P. Poizat, and V. Sandoghdar, J. Microsc. **202**, 2 (2001).
11. T.-P. Vo, M. Mivelle, S. Callard, A. Rahmani, F. Baida, D. Charraut, A. Belarouci, D. Nedeljkovic, C. Seassal, G. Burr, and T. Grosjean, Opt. Express **20**, 4124 (2012).
12. R. Sapienza, T. Coenen, J. Renger, M. Kuttge, N. F. van Hulst, and A. Polman, Nat. Mater **11**, 781 (2012).
13. M. El Kurdi, X. Checoury, S. David, T. P. Ngo, N. Zerounian, P. Boucaud, O. Kermarrec, Y. Campidelli, and D. Bensahel, Opt. Express **16**, 8780 (2008).
14. D. Labilloy, H. Benisty, C. Weisbuch, T. F. Krauss, R. M. De La Rue, V. Bardinal, R. Houdré, U. Oesterle, D. Cassagne, and C. Jouanin, Phys. Rev. Lett. **79**, 4147 (1997).
15. R. Ferrini, D. Leuenberger, M. Mulot, M. Qiu, R. Moosburger, M. Kamp, A. Forchel, S. Anand, and R. Houdré, IEEE J. Quantum Electron. **38**, 786 (2002).
16. B. Lombardet, R. Ferrini, L. A. Dunbar, R. Houdré, C. Cuisin, O. Drisse, F. Lelarge, F. Pommereau, F. Poingt, and G. H. Duan, Appl. Phys. Lett. **85**, 5131 (2004).
17. E. Viasnoff-Schwoob, C. Weisbuch, H. Benisty, S. Olivier, S. Varoutsis, I. Robert-Philip, R. Houdré, and C. J. M. Smith, Phys. Rev. Lett. **95**, 183901 (2005).
18. J. P. Reithmaier, G. Sek, A. Loffler, C. Hofmann, S. Kuhn, S. Reitzenstein, L. V. Keldysh, V. D. Kulakovskii, T. L. Reinecke, and A. Forchel, Nature **432**, 197 (2004).
19. U. Dharanipathy, N. Vico-Trivino, C. Yan, Z. Diao, J. F. Carlin, N. Grandjean, and R. Houdré, Opt. Lett. **37**, 4588 (2012).
20. N. Vico-Trivino, G. Rossbach, U. Dharanipathy, J. Levrat, A. Castiglia, J.-F. Carlin, K. A. Atlasov, R. Butté, R. Houdré, and N. Grandjean, Appl. Phys. Lett. **100**, 071103 (2012).
21. Y.-S. Choi, K. Hennessy, R. Sharma, E. Haberer, Y. Gao, S. P. DenBaars, S. Nakamura, E. L. Hu, and C. Meier, Appl. Phys. Lett. **87**, 243101 (2005).
22. M. Arita, S. Ishida, S. Kako, S. Iwamoto, and Y. Arakawa, Appl. Phys. Lett. **91**, 051106 (2007).
23. M. Mexis, S. Sergent, T. Guillet, C. Brimont, T. Bretagnon, B. Gil, F. Semond, M. Leroux, D. Néel, S. David, X. Chécoury, and P. Boucaud, Opt. Lett. **36**, 2203 (2011).
24. D. Néel, S. Sergent, M. Mexis, D. Sam-Giao, T. Guillet, C. Brimont, T. Bretagnon, F. Semond, B. Gayral, S. David, X. Chécoury, and P. Boucaud, Appl. Phys. Lett. **98**, 261106 (2011).
25. S. Sergent, M. Arita, S. Kako, S. Iwamoto, and Y. Arakawa, Appl. Phys. Lett. **100**, 121103 (2012).
26. D. Sam-Giao, D. Néel, S. Sergent, B. Gayral, M. J. Rashid, F. Semond, J. Y. Duboz, M. Mexis, T. Guillet, C. Brimont, S. David, X. Chécoury, and P. Boucaud, Appl. Phys. Lett. **100**, 191104 (2012).
27. E. Kuramochi, M. Notomi, S. Mitsugi, A. Shinya, T. Tanabe, and T. Watanabe, Appl. Phys. Lett. **88**, 041112 (2006).
28. A. Rodriguez, M. Ibanescu, J. D. Joannopoulos, and S. G. Johnson, Opt. Lett. **30**, 3192 (2005).